Electrochemical Synthesis for the Control of γ-Fe_2O_3 Nanoparticle Size. Morphology, Microstructure, and Magnetic Behavior

C. Pascal, J. L. Pascal, and F. Favier*

LAMMI, ESA 5072 CNRS Université Montpellier II, cc015, Place E. Bataillon, 34095 Montpellier Cedex 05, France

M. L. Elidrissi Moubtassim

LPMC, UMR 5617 CNRS Université Montpellier II, cc03, Place E. Bataillon, 34095 Montpellier Cedex 05, France

C. Payen

IMN, UMR 6502 CNRS Université de Nantes, BP 32229, 44322 Nantes Cedex 03, France

Received August 4, 1998. Revised Manuscript Received October 26, 1998

The electrochemical synthesis of nanoparticles of γ-Fe_2O_3 was performed in an organic medium. The size was directly controlled by the imposed current density, and the resulting particles were stabilized as a colloidal suspension by the use of cationic surfactants. The size distributions of the particles were narrow, with the average sizes varying from 3 to 8 nm. The amorphous character of the nanoparticles was clearly established by X-ray powder diffraction and TEM analysis. The microstructure of this phase could nevertheless be spectroscopically related to maghemite, γ-Fe_2O_3. ^{57}Fe Mossbauer spectroscopy and magnetization measurements indicated that the dry powders exhibit superparamagnetic behavior at room temperature.

I. Introduction

Fundamental as well as technological interest in nanostructured materials is now well-established. The synthesis and characterization of such small objects are the subject of intense current research.[1−5] Furthermore, a wide variety of applications, particularly in the field of catalysis and especially those involving nanoparticles, is now an industrial reality.[6,7] The improved reactivity of nanoparticles is associated with the high ratio of surface area to volume.

Small particles, with diameters less than 10 nm, exhibit material properties which strongly differ from those of bulk phases. Their electronic, magnetic, and optical properties contribute attractive prospects in the design of new electronic and optical devices, information storage, color imaging, bioprocessing, magnetic refrigeration, ferrofluids, gas sensors, etc.[8−12] In these latter fields of application, small particles of metal oxide are particularly important.[13]

Numerous methods for the synthesis of metal oxide nanoparticles have been reported.[3] Various compositions and morphologies have been obtained by oxyhydrogen flame pyrolysis,[14] sol−gel processes,[15,16] chemical oxidation in micellar media or in polymer or mineral matrixes,[17] etc. The amorphous character of the prepared material is one of the main parameters requiring control. Moreover, the extent of amorphous character of a solid is a concept only recently considered. Amorphous metal oxides are generally obtained by the decomposition of chosen precursors with a high cooling rate up to 10^5−10^7 K s^{-1}.[14,18] To our knowledge, "chimie douce" (soft chemical) preparative methods for amorphous oxides are currently limited to sol−gel processes and to precipitation in strong basic medium of chosen precursors.[19]

(1) Ziolo, R. F.; Giannelis, E. P.; Weinstein, B. A.; O'Horo, M. P.; Ganguly, B. N.; Mehrotra, V.; Russel, M. W.; Huffman, D. R. *Science* **1992**, *257*, 219.
(2) Ozin, G. A. *Adv. Mater.* **1992**, *4*, 612.
(3) Matijevic, E. *Chem. Mater.* **1993**, *5*, 412.
(4) Reetz, M. T.; Helbig, W.; Quaiser, S. A. In *Active Metals: Preparation, Characterization, Applications*; Fürstner, A., Ed.; VCH: Weinheim, 1996 and reference therein.
(5) Barbé, C. J.; Arendse, F.; Comte, P.; Jirousek, M.; Lenzmann, F.; Shklover, V.; Grätzel, M. *J. Am. Ceram. Soc.* **1997**, *80*, 12, 3157.
(6) Conway, B.; Tilak, B. In *Advanced Catalysis;* Eley, D., Pines, H., Weisz, P., Eds.; Academic Press: New York, 1992.
(7) Cao, H.; Suib, S. L. *J. Am. Chem. Soc.* **1994**, *116*, 5334.
(8) Shön, G.; Simon, U. *Colloid Polym. Sci.* **1995**, *273*, 101.
(9) Günther, L. *Phys. World* **1990**, *3*, 28.
(10) Ziolo, R. F. U.S. Patent 4,474,866, **1984**.
(11) Nixon, L.; Koval, C. A.; Noble, R. D. *Chem. Mater.* **1992**, *4*, 117.
(12) Anton, I. *J. Magn. Magn. Mater.* **1990**, *85*, 219.
(13) Livage, J. *J. Phys. Chem.* **1981**, *42*, 981.
(14) Grimm, S.; Schultz, M.; Barth, S.; Müller, R. *I. Mater. Sci.* **1997**, *32*, 1083.
(15) Stöber, W.; Fink, A.; Böhn, E. *J. Colloid Interface Sci.* **1968**, *26*, 62.
(16) Jean, J. H.; Ring, T. A. *Langmuir* **1986**, *2*, 251.
(17) Mounien, N.; Pileni, M. P. *Chem. Mater.* **1996**, *8*, 1128.
(18) Cao, X.; Koltypin, Yu; Prozorov, R.; Kataby, G.; Gedanken, A. *J. Mater. Chem.* **1997**, *7*, 12, 2447.
(19) Inskeep, W. P. *J. Environ. Qual.* **1989**, *18*, 379 and references therein.

10.1021/cm980742f CCC: $18.00
Published on Web 12/15/1998

On the other hand, although the preparative routes for small particles have greatly improved in the past decade, they have also revealed two synthetic challenges: (i) the particle size should be controlled during the synthesis and the polydispersity of the size distribution should be narrow and (ii) particle agglomeration should be prevented (aggregated nanoparticles do not remain nanoparticulate).

In this paper, we present an electrochemical synthesis of γ-Fe_2O_3 nanoparticles less than 10 nm in size and meeting both these requirements. The particle size is controlled by adjusting the imposed current density while absorbed long chain tetraalkylammonium salts prevent particle aggregation in organic media. Morphology and microstructure are discussed on the basis of TEM measurements, X-ray diffraction, and vibrational analysis. Since a few studies have been devoted to the magnetic properties of particles of maghemite iron(III) oxide on the nanometric scale, the magnetic behavior of the dry fine powders is described.

II. Experimental Section

A sacrificial iron anode (3 cm^2, 2 mm thick) was purchased from Goodfellow (99.5%), while the cathode was a platinum foil (5 cm^2, 0.5 mm of thickness). The distance between these two electrodes was restricted to less than 1 cm. The supporting electrolytes were 0.05−0.15 M solutions of tetraoctylammonium bromide (Fluka, 98%) in *N*,*N*-dimethylformamide (DMF, Aldrich, ACS reagent). Less than 5% in volume of demineralized water was added to the solution. The applied current densities varied from a few mA cm^{-2} to a few tens of mA cm^{-2} for a corresponding potential from 1.8 to 4 V (versus the platinum counter electrode). At room temperature and at these values of potential, up to the normal potential of H_2O, the water is anodically oxidized. During the electrolysis, the formation of brown precipitates was observed. The precipitates were washed with DMF and centrifuged several times to remove the excess of $(octyl)_4NBr$. The concentrated suspensions (<50 g/L) in DMF of $Fe_2O_3 \cdot \epsilon(octyl)_4NBr$, with $0.07 < \epsilon < 0.1$, were kept stable for several days. Powders were dried in air at 340 K before characterization. The absence of Fe^{2+} ions was confirmed by potassium bichromate titration.[20]

Transmission electron microscopy studies and electron diffraction were carried out with a JEOL 1200 EX2 microscope. Powders were dispersed on Collodion grids from butanol suspensions. The histograms of size distributions were obtained by measuring the diameter, D_i, of at least 200 particles. The standard deviation, σ, is given by the following relation:

$$\sigma = [\sum (N_i(D_i - D)^2)/(N - 1)^2]^{1/2}$$

where D and N are respectively, the average diameter and the number of particles.

X-ray powder diffraction patterns were obtained using Cu Kα radiation on an automatized Philips PW1965/30 goniometer.

IR spectroscopic characterization was carried out using a FTIR BOMEM DA8 spectrometer. Sampling was done in KBr.

Raman spectra were recorded on a LABRAM-Dilor spectrometer. Powders were sampled on a glass plate, while a HeNe laser (632.817 nm, 20 mW) was focused using a BX40 microscope (magnification ×50).

BET surfaces were determined by N_2 absorption. Powders were evacuated for 12 h at 373 K under secondary vacuum (0.1 mPa). Absorption isotherms were recorded using a Sorptomatic 1900 apparatus.

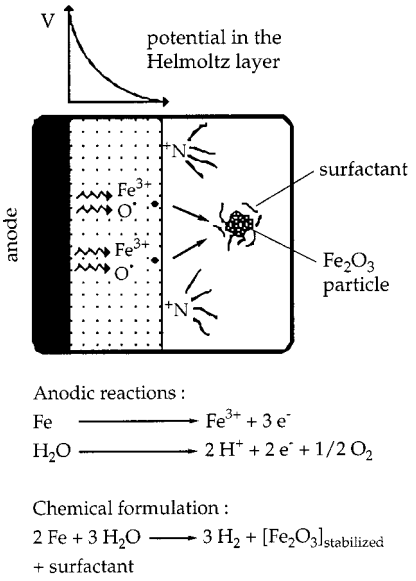

Figure 1. Formation of stabilized Fe_2O_3 nanoparticles.

^{57}Fe Mössbauer transmission spectra were recorded at room temperature and 77 K in the constant-acceleration mode between −12 and 12 mm s^{-1}. At room temperature, only a doubletlike signal is observed with no additional bands outside the −3 to 3 mm s^{-1} range. The room-temperature spectrum was therefore recorded within this velocity range. The velocity scale was calibrated with the magnetic sextet spectrum of a high-purity iron foil absorber. To avoid any side line-broadening due to the isotopic thickness effect, the dry powders were dispersed in Apiezon grease with respect to 1 mg cm^{-2} ^{57}Fe concentration which have been previously tested for other known compounds to give usual line widths. Sampling was carried out between two transparent iron-free foils. Recorded spectra were fitted using Lorentzian profiles by the procedure described by Lecaer.[21]

Magnetic studies were done on dry powders using a SQUID magnetometer (MPMS5.5, Quantum Design). The magnetic susceptibility of $(C_8H_{17})_4NBr$ was found to be very weak, -7×10^{-6} emu/g, corresponding to less than 0.1% of the total magnetic moment of the material. Relative magnetization M/M_s curves were fitted with the Langevin relationship:[22]

$$M/M_s = \coth(\mu H/kT) - kT/\mu H \quad (1)$$

where M_s is the saturation magnetization of the sample and $\mu = M_s \pi D^3/6$, with M_s being the saturation magnetization of the bulk phase. A log-normal distribution of the particle sizes was assumed for calculations.

III. Results and Discussion

Reetz et al. have recently developed an electrochemical synthesis of nanosized metal clusters.[4] Although this method is limited to metal alloy particles, they have clearly demonstrated the powerful potential of such a preparative route.

Our method is based on the same kind of generation of metal cations in organic medium from a sacrificial anode. The value of the electrolysis potential is sufficiently high to allow the anodic oxidation of water present in small amounts in solution. The resulting

(20) The iron oxide was dispersed in water previously boiled to remove the oxygen. Concentrated hydrochloric acid was added and dissolution occurred at reflux under nitrogen flow. Iron(II) content was determined by titration with a potassium bichromate solution with diphenylamide barium as the indicator.

(21) Lecaer, G.; Dubois, J. M. *J. Phys. E: Sci. Instrum.* **1979**, *12* (11), 1083.

(22) Charles, S. W.; Popplewell, J. In *Ferromagnetic Materials*; Wohlfarth, H., Ed.; North-Holland Publishing: Amsterdam, 1982; Vol. 2.

Table 1. Average Particle Size (nm) by TEM, D_{TEM}, and by Magnetic Measurements, D_{magn}, and Coercivity, H_c (Oe), and Reduced Remanence M_r/M_s at Room Temperature

applied density/mA cm^{-2}	D_{TEM}	D_{magn}	H_c	M_r/M_s
1.5	7.4	nd[a]	nd	nd
3	6.0	8.3	4	0.009
8	5.5	7.4	2	0.005
12	4.8	nd	nd	nd
17	3.8	5.6		
25	3.2	nd	nd	nd

[a] nd = none determined.

reactive oxygen complexes the metal cations to give the corresponding metal oxide. A tetraalkylammonium type surfactant, which also plays the role of electrolyte, stabilizes the resulting small particles. As depicted in Figure 1, all the stages of the reaction take place at the anode or close to it: the production of iron cations and "O•" species, the complexation, and the stabilization. In view of the stoichiometry of the resulting oxide, Fe_2O_3, it can be assumed in the global chemical formulation that mainly Fe^{3+} cations are anodically produced. The cogeneration of Fe^{2+} ions could also occur, but these are oxidized in situ by the coproduced oxygen species.

A first preparation was performed in a 0.05M solution of $(octyl)_4NBr$ in DMF and using a 1.5 mA cm^{-2} current density for a corresponding potential of 2.03 V. The mean particle size was determined by TEM image analysis to be 7.4 nm (Table 1). To determine whether the current density has any effect upon the particle size and size distribution, a series of preparations was carried out using current densities varying from 3 to 8, 12, 17, and 25 mA cm^{-2}. To prevent an undesired oxidation of the solvent, the corresponding potential was controlled by the concentration in tetraalkylammonium salt and limited to at least 3 V. The product observed by TEM (Figure 2), had, for all the current density, the appearance of formless, nonfaceted particles not resembling crystallites. The histogram in Figure 3 clearly confirms the relationship between the applied current density and the mean size of these particles measured by TEM. The greater the imposed current density, the smaller the particle size. The histograms of the size distribution are shown in Figure 4. In all cases, the size distribution is rather narrow with a standard deviation of about 20%. The observed dispersity can also be correlated to the current density: at low applied density, the monodispersity is less. This small size and narrow dispersity are due to the thickness of the Helmoltz layer and the high diffusional rates, confirming that agglomeration before stabilization is limited.

The choice of the type of tetraalkylammonium surfactant is governed by two constraints: (i) it should be adsorbed on the metal oxide surface to stabilize the synthesized nanoparticles and (ii) it should be highly soluble and dissociated in the solvent to play the role of electrolyte. Moreover, due to the presence of water, even in small quantities in the medium, the hydrophilic−lipophilic balance (HLB) of the chosen surfactant should be sufficiently high to prevent any precipitation.

One of the main features of this preparative route is that the particles are dispersed in an organic medium. Of course, the synthesized oxide should be insoluble in the chosen solvent. DMF is used for the electrolysis, but

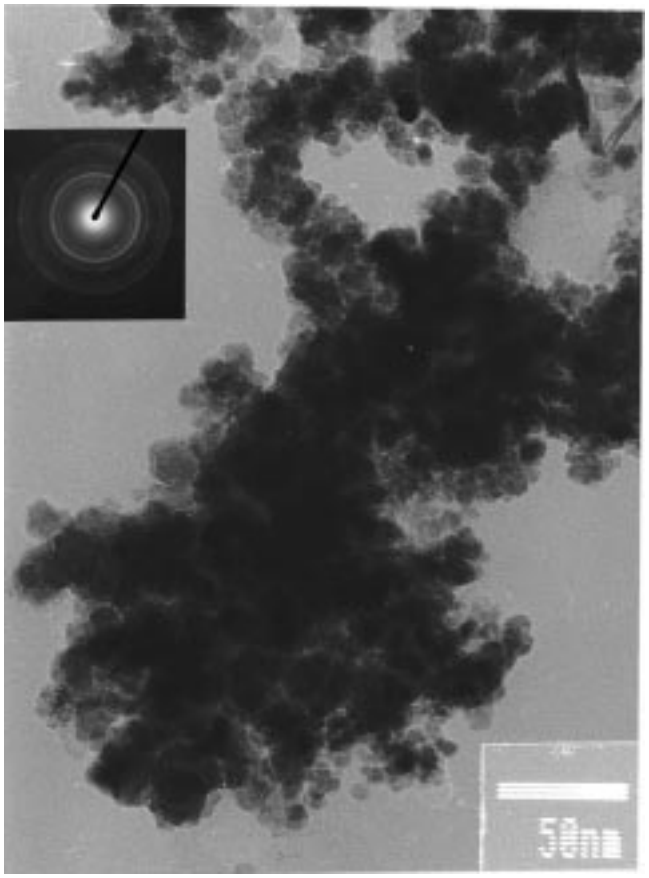

Figure 2. TEM image of γ-Fe_2O_3 nanoparticles prepared at 3 mA cm^{-2} in DMF. The insert shows the corresponding electron diffraction pattern.

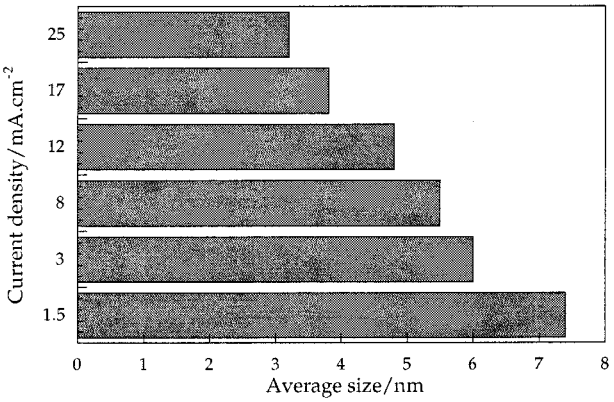

Figure 3. Distribution of averaged size for particles obtained at various current densities.

stable colloidal suspensions can also be obtained in numerous common solvents such as THF, DMSO, or long chain alcohols, by redispersion of the dried powders. The use of apolar organic solvents such as toluene is also possible. In this case, the cationic surfactant allows the solubilization of the water. These nanoparticles can also be dispersed in situ and immobilized in mineral (SiO_2, Al_2O_3, etc.) or polymer matrixes introduced into the electrolysis cell as suspensions or solutions, respectively.

Whatever the value of the applied current density, the X-ray diffraction pattern of the resulting iron oxide was characteristic of an amorphous phase. The X-ray diffraction patterns of some samples showed lines characteristic of crystallized tetraoctylammonium bro-

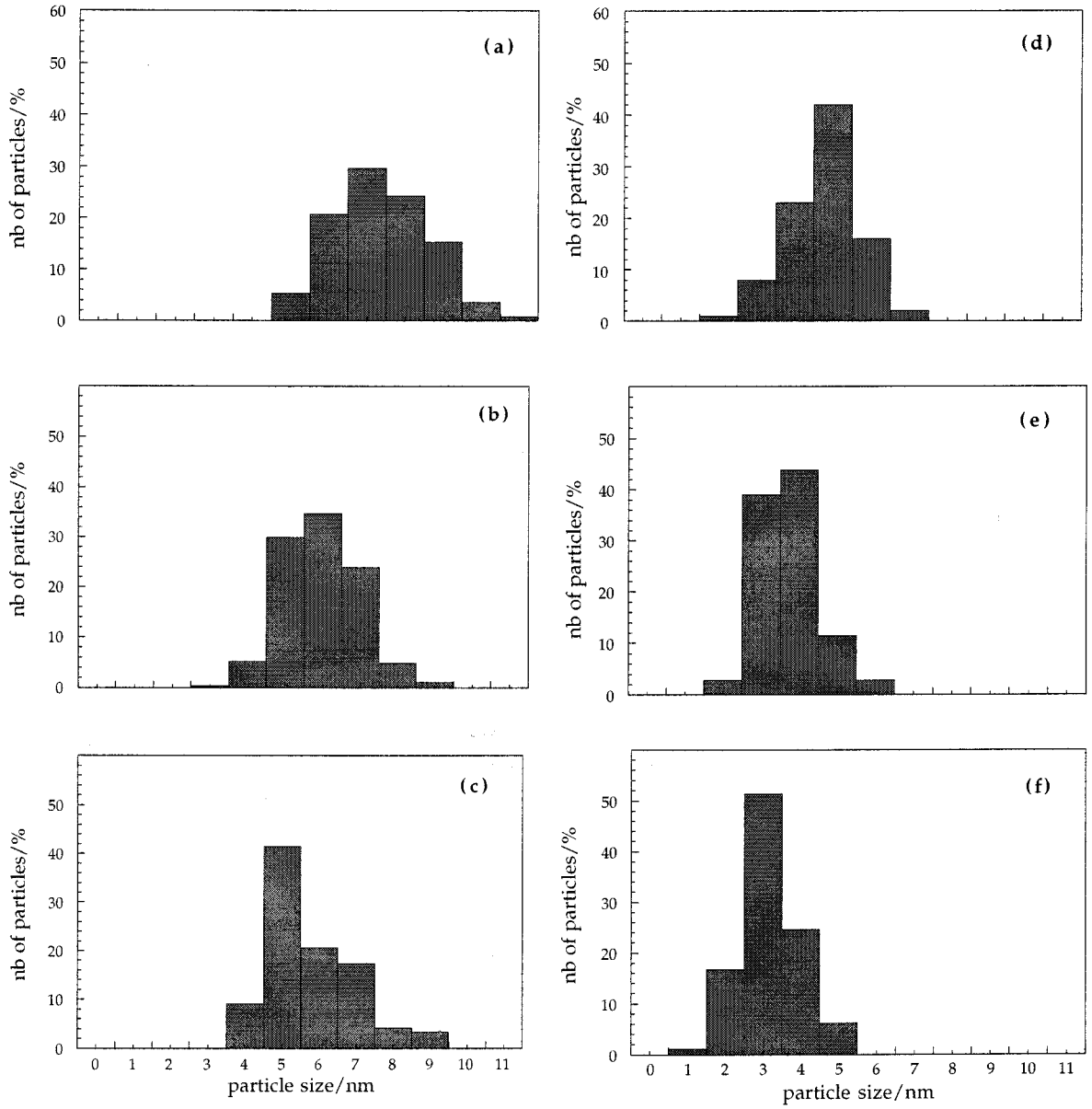

Figure 4. Histograms of size distribution. Imposed current density is (a) 1.5 mA cm^{-2}, (b) 3 mA cm^{-2}, (c) 8 mA cm^{-2}, (d) 12 mA cm^{-2}, (e) 17 mA cm^{-2}, and (f) 25 mA cm^{-2}.

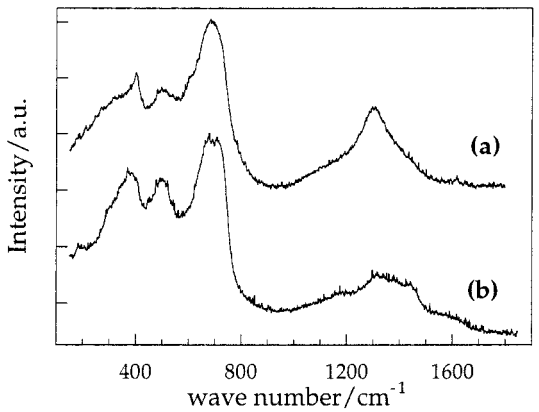

Figure 5. Raman spectra of γ-Fe_2O_3 powders prepared at 1.5 mA cm^{-2} (a) and 25 mA cm^{-2} (b).

mide. These lines disappear on further washing with DMF. An FTIR investigation carried out between 400 and 4000 cm^{-1} confirmed the adsorption of tetraoctylammonium species on the surface of the Fe_2O_3 particles [ν/cm^{-1}: 1031−1102 (w), ν_{C-C} and ν_{N-C}; 1386−1466 (m), δ_{C-H}; 2844−2915 (s), ν_{C-H}]. This absorbed surfactant can be removed by slow thermolysis at 450 K under vacuum (1.33 Pa). Under these conditions, annealing effects are still limited and no phase transformation occurs.

Figure 5 shows the Raman spectra between 200 and 1850 cm^{-1} of the powders prepared at 2 and 17 mA cm^{-2}. These spectra are similar to each to other and suggest that, under the operating conditions used in this work, γ-Fe_2O_3 was the phase which was systematically obtained. These spectra are very close to those of maghemite, γ-Fe_2O_3, reported by Thierry[23] and more recently by de Faria.[24] When the laser beam was focused on a small surface (less than 10 μm^2) in the absence of an appropriate filter, two additional strong Raman lines appeared between 200 and 300 cm^{-1}. These are char-

(23) Thierry, D.; Persson, D.; Legraph, C.; Delichere, D.; Joiret, S.; Pallota, C.; Hugot-Legoff, A. *J. Electrochem. Soc.* **1988**, *135*, 305.
(24) De Faria, D. L. A.; Venâncio Silva, S.; de Oliviera, M. T. J. *Raman Spectrosc.* **1997**, *28*, 873.

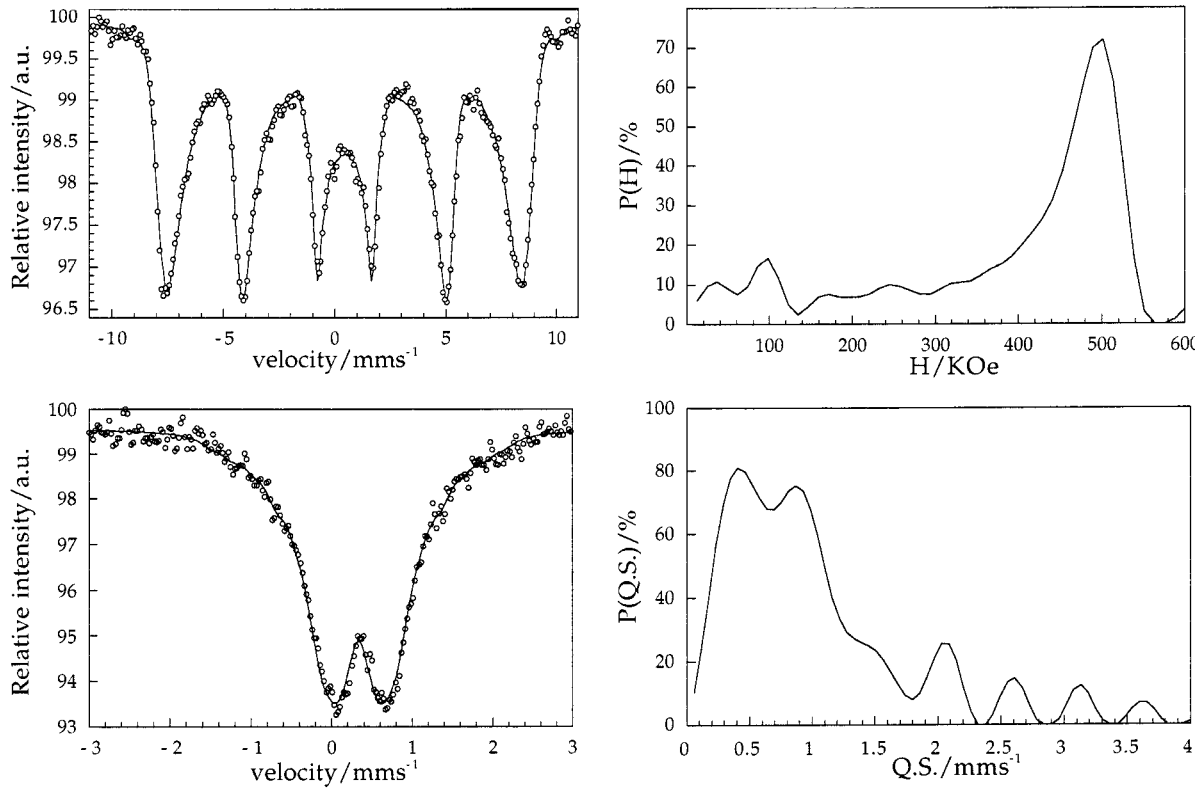

Figure 6. Experimental (open circle) and calculated (solid line) Mössbauer spectra of 3.8 nm particles at room temperature (bottom) and at 77 K (top). The corresponding distribution of electric field gradients and of internal magnetic fields respectively are also given.

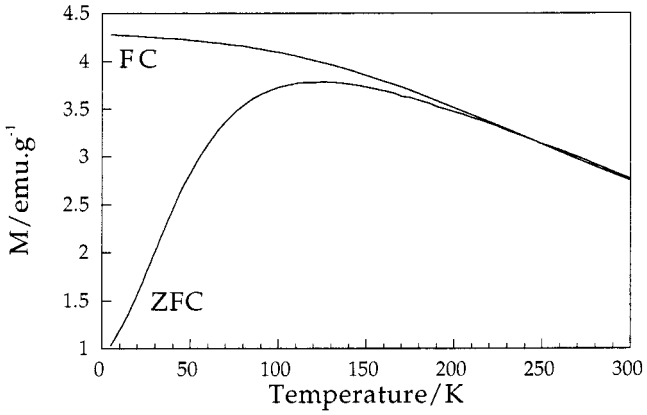

Figure 7. Temperature dependence of the magnetization in the ZFC and FC cases with applied field H = 100 Oe for particles of 3.8 nm.

acteristic of the well-known phase transformation from maghemite to hematite, α-Fe_2O_3, at temperatures varying from 640 to 870 K, depending on the particle size. Therefore to obtain the spectra presented in Figure 5, a beam generating a very low heat was used. The prepared amorphous iron oxide can thus spectroscopically be related to maghemite in terms of the short-range atomic order of the oxygen atoms around iron. This relationship was confirmed by electron diffraction carried out on samples in the electron microscope, which produced a series of diffuse diffraction ring despite the absence of peaks in the X-ray powder diffraction. The most intense diffraction rings correspond to those of maghemite (insert Figure 2).

N_2 adsorption−desorption isotherm curves were established for two samples of γ-Fe_2O_3 powders prepared at 3 and 17 mA cm^{-2}. These isotherm curves are of type II and are characteristic of a nonporous material. The Cranston and Inkley method[25] confirmed that the overall surface is external. The corresponding BET surface areas were respectively 40 (C = 26.9) and 48 (C = 23.9) m^2 g^{-1}. These values are in good agreement with those reported in the literature.[26]

The room-temperature Mössbauer spectrum of dry powder with 3.8 nm particles consists of a like-splitted line with a large width, in agreement with the amorphous state characterized by X-ray diffraction. The fitting procedure is therefore based on a quadrupolar splitting distribution arising from the electric field gradient distribution encountered in such amorphous materials. Figure 6 shows the experimental and calculated spectra and the resulting quadrupolar splitting distribution. The corresponding hyperfine parameters are δ = 0.33 mm s^{-1}, $\langle$QS$\rangle$ = 1.00 mm s^{-1}, which are typical of iron(III).[27] The spectrum recorded at 77 K consists of a broadened sextet, fitted with the same procedure with respect to the internal magnetic field distribution. Experimental and calculated spectra are depicted in Figure 6. In this case the isomer shift is 0.44 mm s^{-1} and the mean internal field is 386 kOe. Differences between room and low-temperature isomer shifts are due to the thermal variation of the second-order Doppler effect.[28] The appearance of a magnetic

(25) Cranston, R. W.; Inkley F. A. *Adv. Catalysis* **1957**, *9*, 143.
(26) Cornell, R. M.; Schwertmann, U. In *Iron Oxides*; VCH: Weinheim, 1996; p 87.
(27) Da Costa, G. M.; De Grave, E.,; Bowen, L. H.; Vandenberghe, R. E.; de Bakker, P. M. A. *Clays Clay Min.* **1994**, *42*, 628.
(28) Chantrell, R. W.; Popplewell, J.; Charles, S. W. *Physica* **1977**, *86−88B*, 1421.

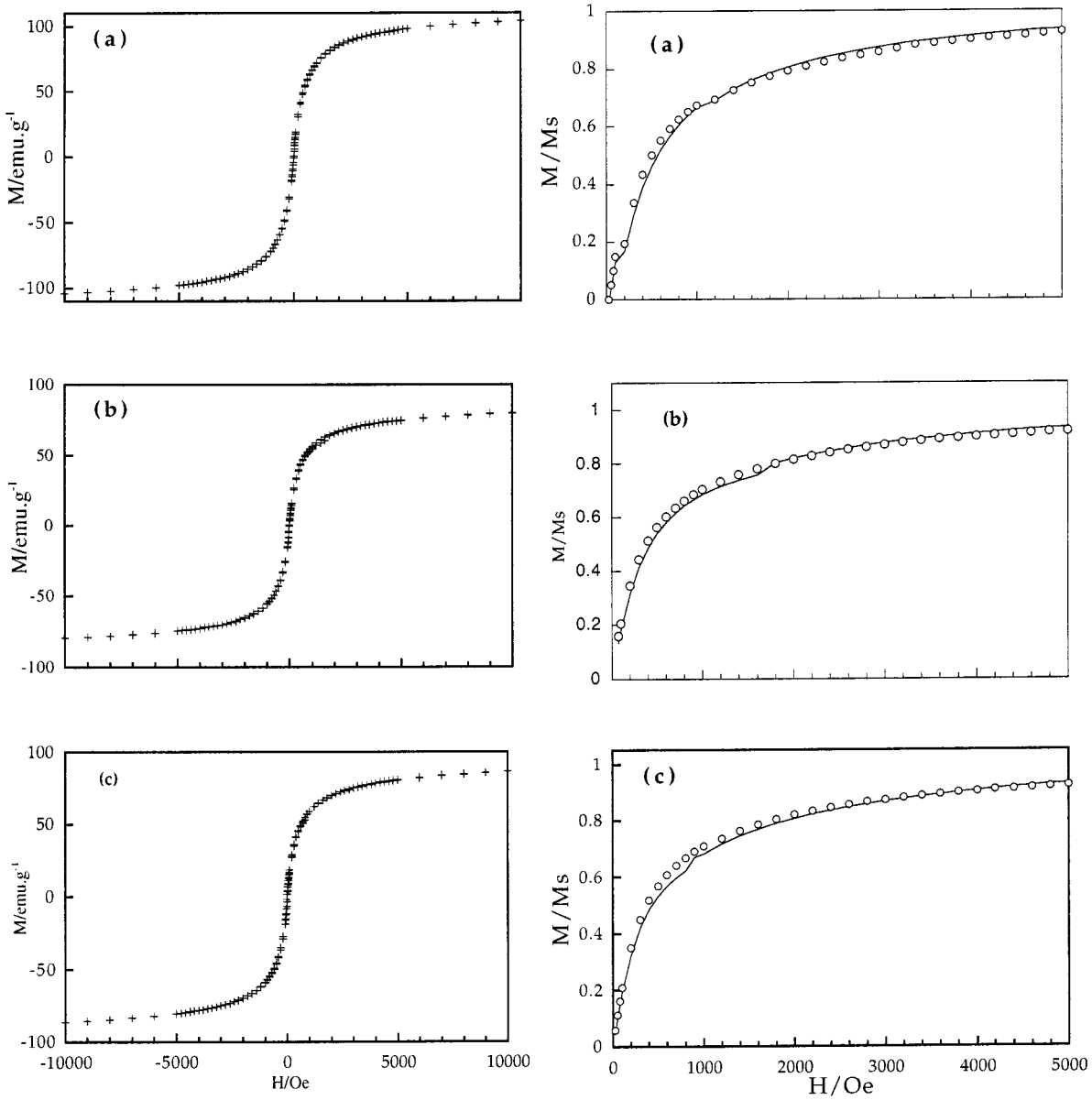

Figure 8. Experimental (cross and open circle) and calculated (solid line) curves of relative magnetization as a function of applied field at room temperature. Particle size: 6.0 nm (a), 5.5 nm (b), and 3.8 nm (c).

splitting at low temperature is due to a blocking of superparamagnetic fluctuations, as suggested previously.[29]

Superparamagnetism is often observed for particles below about 10 nm. The occurrence of superparamagnetic behavior is confirmed by the temperature and field dependences of the magnetization that we observed for dry powders. Figure 7 shows the thermal variation of the magnetization measured for a 3.8 nm sample with an applied magnetic field of 100 Oe. These data were recorded in the temperature range 5−300 K using the standard zero-field-cooling (ZFC) and field-cooling (FC) procedure. The ZFC/FC irreversibility and the broad maximum in the ZFC curve are expected for superparamagnetic particles. The temperature at which the ZFC curve exhibits a cusp is defined as the blocking temperature (TB). Below TB, the superparamagnetic transition is blocked, i.e., the magnetization cannot relax during the time of the measurement. From our data, TB = 125(5) K for $H = 100$ Oe. This value is very close to those reported for a ferrofluid sample with averaged particle diameter of 5 nm: TB = 140 K for $H = 100$ Oe.[30,31] Above TB, the magnetization should be free to align the field during the measurement time, and the curves of magnetization versus applied field should exhibit no hysteresis loop. In this superparamagnetic state, the magnetization is described by the Langevin function (eq 1).

We therefore recorded room-temperature isothermal magnetization curves for 3.8, 5.5, and 6 nm powders. Closed $M-H$ loops are indeed observed (Figure 8). Furthermore, as expected from the Langevin relationship, the magnetization saturation is reached at a higher magnetic field for the smallest particle sizes.

(29) Morup, S.; Tronc, E. *Phys. Rev. Lett.* **1994**, *72*, 3278.

(30) Zhang, X. X.; Ziolo, R. F.; Kroll, E. C.; Bohigas, X.; Tejada, J. *J. Magn. Mater.* **1995**, *140−144*, 1853.

(31) Tejada, J.; Ziolo, R. F.; Zhang, X. X. *Chem. Mater.* **1996**, *8*, 1784.

Assuming a log-normal size distribution of superparamagnetic particles, their "magnetic" size can be calculated from the Langevin relationship. Figure 8 shows a good agreement between experimental and simulated relative magnetization M/M_s curves as a function of the applied magnetic field. The corresponding values of "magnetic" size (Table 1) are overestimated by about 40% in comparison with the sizes evaluated by TEM. These differences, previously observed in dry fine powders,[17] can be attributed to weak interactions between particles. Due to a perturbation in the Langevin curve, such interactions induce an apparent "magnetic" size larger than those measured by TEM.

IV. Conclusion

The size, ranging from 3 to 8 nm, of particles of maghemite, γ-Fe_2O_3, can be controlled by an electrochemical preparation method. The particles are stabilized in organic medium by adsorption of cationic surfactants. The Fe_2O_3 particles prepared by this "chimie douce" method are X-ray amorphous but are identified as γ-Fe_2O_3 by Raman spectroscopy and electron diffraction. Dry powders of this material exhibit superparamagnetic behavior.

CM980742F